Haptics-e, Vol. 4, No. 3, July 21, 2006
http://www.haptics-e.org

THE COMMON PATTERNS OF BLOOD PERFUSION IN THE FINGERNAIL BED SUBJECT TO FINGERTIP TOUCH FORCE AND FINGER POSTURE

Stephen A. Mascaro
Department of Mechanical Engineering
University of Utah
smascaro@mech.utah.edu

H. Harry Asada
Department of Mechanical Engineering
Massachusetts Institute of Technology
asada@mit.edu

ABSTRACT

When the human fingertip is pressed against a surface or bent, the hemodynamic state of the fingertip is altered in a way that is common to all people. Normal force, shear force, and finger extension/flexion all result in visibly distinct patterns of blood volume or perfusion beneath the fingernail. These patterns of blood perfusion can be used not only to monitor the state of the finger, but also to understand how the fingernail interacts with the bone and surrounding tissues when various forces or postures are applied.

In this paper, photographic techniques are used to catalog the average patterns of fingernail coloration corresponding to various states of applied forces and postures across human subjects of a variety of size, gender, and skin color. Results indicate that there are at least seven different states of force and posture that yield distinct coloration patterns that are statistically significant and common to people in general.

1. INTRODUCTION

There is an increasing interest in understanding fingertip forces in the growing fields of haptics and virtual reality, in addition to more established fields such as robotics and medicine [1]. These forces act as bi-directional feedback between human and environment, either mechanical or virtual. Forces applied by a machine or virtual tool are fed back and presented to the human, while forces applied by the human are measured and fed back to the machine or virtual environment. Both application and measurement of fingerpad forces are required, and understanding the mechanics and dynamics of the human fingerpad is important for both.

Several researchers have investigated the mechanics and dynamics of the human fingerpad [2-5]. Resulting analyses lead to a better understanding of human grasping and manipulation, characterizations of the human haptic sense, ergonomic design criteria [2,3], and performance criteria for haptic feedback devices [6]. However only a few studies have taken into account the role of the fingernail in fingerpad behavior [7]. It is well documented in medical literature that the fingernail plays an important role in grasping and fine manipulation [8,9].

In addition to applying forces, the fingernail has recently been discovered to be useful for measurement of forces. When forces are applied to the fingerpad, interaction between the fingernail, bone, and tissue alters the hemodynamic state of the finger, creating various patterns of blood volume or perfusion in the capillaries beneath the fingernail. In previous work, photoplethysmograph fingernail sensors have been designed which optically measure the two-dimensional pattern of blood perfusion beneath the fingernail [10]. These patterns can then be used to estimate the fingerpad forces and finger posture.

In order to better design such fingernail force sensors, it is important to understand the sensing mechanism, including the mechanics of the fingernail-bone-tissue interaction and its effect on blood perfusion. In previous research, the mechanism behind the hemodynamic response to normal force has been quantitatively modeled, but the response to shear force and finger bending were not understood [11]. It was suspected that normal forces, shear forces, and changes in finger posture all result in measurably different blood perfusion patterns that are (to some degree) common to all people. Up until now, this has not been substantiated.

In this paper, the observable fingernail color patterns that are representative of blood perfusion are cataloged for a variety of human subjects in response to a variety of force and posture states or poses. Photographic results are combined to create a set of "average" patterns that apply to all subjects. The patterns from all the subjects are correlated to these average patterns to determine whether the average patterns can be used to classify the responses of all people in a statistically significant manner. Finally, important outcomes are discussed, including HCI applications as well as unified modeling of fingertip behavior during touching and grasping.

2. FINGERNAIL COLOR PATTERNS

As the human fingertip is pressed down on a surface or bent, the blood perfusion in the fingertip is affected. In fact, the change in blood perfusion is characteristically non-uniform across the nail, resulting in distinct patterns of red and white fingernail coloration for different types of forces and posture. Figure 1 shows the primary variables of interest that affect the coloration of the fingernail. These include the normal force, F_z, the lateral shear force, F_x, and the longitudinal shear force, F_y, which occur when the finger is pressed against a surface. Since the finger surface is curved, the direction of force and its influence on coloration vary depending on the location, contact angle, and contact surface shape. This paper focuses on the case where the fingerpad is pressed against a large, uniformly flat surface parallel to the bone of the distal phalanx, such that the contact area is maximized and the contact is most stable. Thus the contact location is standardized and the three touch force directions are defined with respect to the surface.

Also of interest are the three posture angles, J_1, J_2, and J_3. However, in practice J_1 does not affect the fingernail color; also J_3 is coupled to J_2 as long as the finger is not in contact with the surface when bending occurs. Therefore, in this paper the only posture angle of interest is J_2, hereafter referred to as θ.

There are many other variables that may affect blood perfusion in the fingertip such as body or finger temperature, hand elevation, or any other factors affecting blood pressure or cardiovascular activity. In this paper, experiments are conducted with the body at rest in a constant temperature environment with the hand at constant desk level in order to minimize the effects of any such variables.

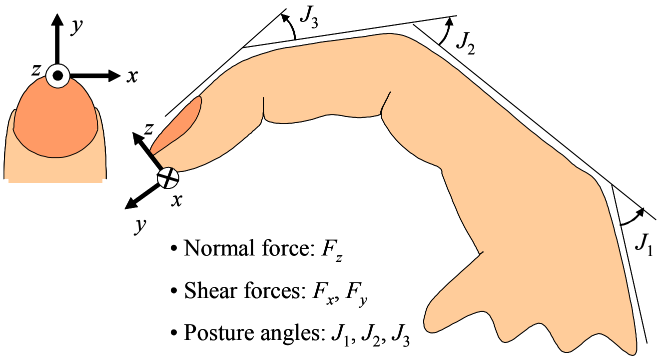

Figure 1. Finger variables of interest. The forces are defined to be positive when the finger is pressed against a surface in the positive *x*, *y*, and *z* directions as shown. The finger posture is represented by the angle of the knuckle (MP) joint, J_1, the middle (PIP) joint, J_2, and the distal (DIP) joint, J_3. The angles are defined to be positive for flexion and negative for extension.

In this study, digital images were collected for 15 human subjects: 10 male and 5 female. For purposes of categorizing skin color, 7 subjects were white, 7 were Asian, and 1 was black. In order to uniformly photograph the subjects, an apparatus was designed as shown in Figure 2. A 3-axis force-sensing platform with rubber surfaces is placed within an enclosed chamber to block ambient lighting. A 1.0 MegaPixel CCD digital camera with 10x optical zoom is mounted above the force-sensing platform in order to image the fingernail as the finger is pressed against the platform with various forces or held with various postures. The human subjects use visual feedback from the force sensor to maintain constant desired force. The two key features of the apparatus are the lighting and the filtering. First, in order to prevent glare from ruining the image, the light must be placed directly behind the fingernail, over the hand, as shown in the figure, so that the curvature of the nail will reflect the light out away from the lens. In this situation, the only light that reaches the lens is the light that penetrates the nail bed and is diffusively reflected back out. Second, when sample images are broken down into their RGB (red-green-blue) components, results show that the visibly "red" and "white" areas of the fingernail differ principally in their green component, which can be isolated (by software or hardware filters) to generate a high-contrast grayscale image.

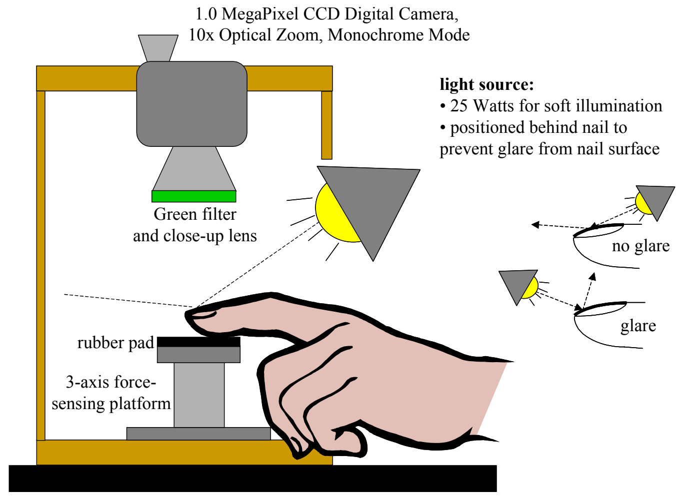

Figure 2. Experimental apparatus. A CCD camera images the fingernail coloration while the finger is pressed against the force platform with specified force.

All 15 subjects were photographed in eight different poses. The first image is the nominal coloration of the fingernail when no force is applied and the finger is held straight out. For the second image, a normal force of -3 N is applied. Then lateral and longitudinal shear forces of negative and positive 2 N are added. Finally, images are taken of the finger fully extended and fully flexed with no force applied. These poses are near the limits of steady-state force/posture that can be comfortably maintained (on the order of a minute), and are also near the saturation limits of the fingernail coloration effect [10] where the coloration is insensitive to small fluctuations in force/posture due to unsteady control by the subjects.

In order to compile the images for all 15 subjects into meaningful results for any particular pose, the intensity values are averaged across all the subjects, resulting in an "average" fingernail image depicting the average pattern of coloration. First, the sizes of the images are normalized according to the length and width of the fingernail. The length is defined as the maximum distance in the y-direction from the eponychium (where the nail emerges from the proximal nail fold) to the hyponychium (where the nail separates from the distal bed), and the width is defined as the maximum distance in the *x*-direction between the lateral nail folds. Then the images are uniformly cropped about the center of the nail to 125% of the normalized nail size, leaving a small area visible around the nail. The resulting images are all 400x400 pixels, with a 320x320 pixel fingernail in the center. Finally, the intensity value for each pixel is averaged across the 15 subjects.

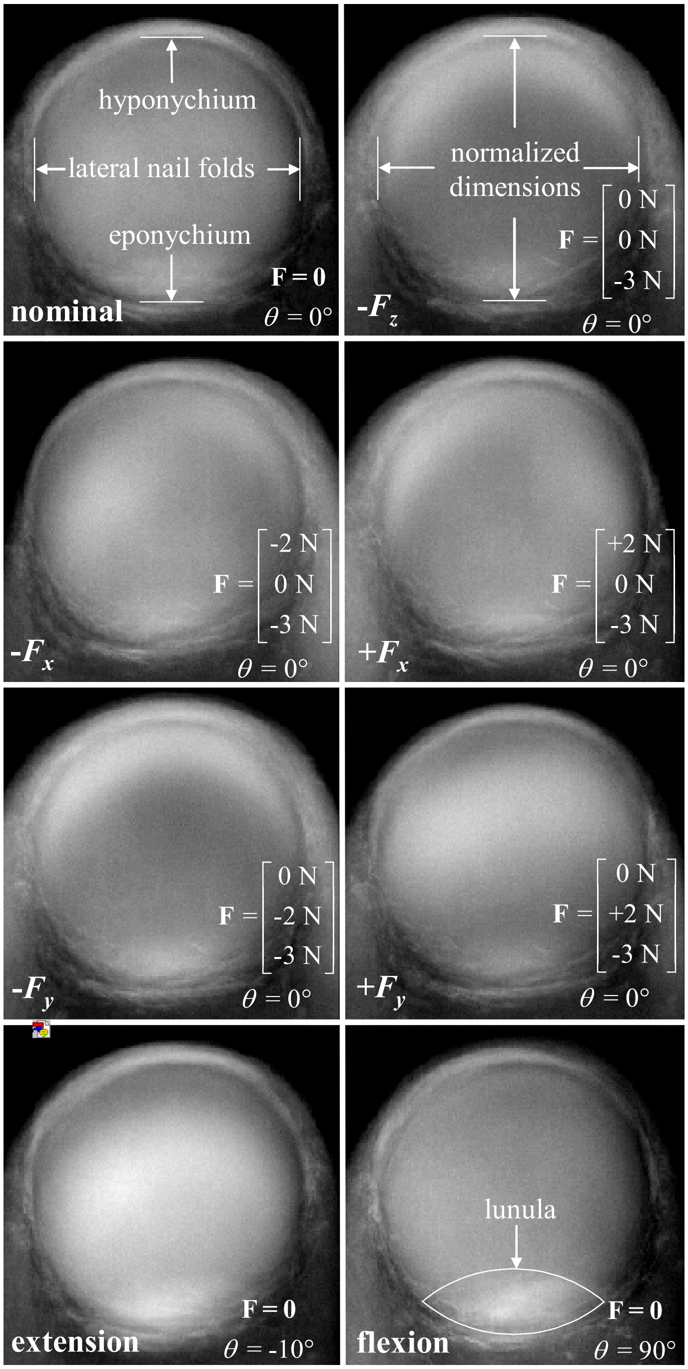

Figure 3. Average fingernail coloration for 15 human subjects for various poses. Images from the 15 subjects were normalized to the same size and averaged pixel by pixel. 5x contrast is applied. Subjects were instructed to apply the same constant forces using visual feedback from the force sensor.

The results are shown in Figure 3. As evidenced in the figure, the various poses result in visibly different average patterns of coloration with well-defined dark and white zones, corresponding to the red and white areas, respectively, of the fingernail. The lunula (visible portion of the nail matrix) appears as a grayish-white zone that varies in size and thus is not useful for establishing commonality between subjects.

3. ANALYSIS

In order to evaluate whether these average patterns are distinct in a statistically significant sense, all of the images for each pose should be correlated to a standard set of images that is representative of the common pattern for each pose. The logical choice for such a standard set of images is the set of average images in Figure 3. For example, if the images of all the subjects for $+F_x$ correlate best in a statistically significant sense to the average image for $+F_x$ compared to the average images for the other poses, then it can be concluded that the response to $+F_x$ is common for all subjects and distinct from all other poses. Moreover, if this is true for all poses, then it will have been demonstrated that there is a set of common distinct patterns (namely the set of images in Figure 3) that is representative of all subjects.

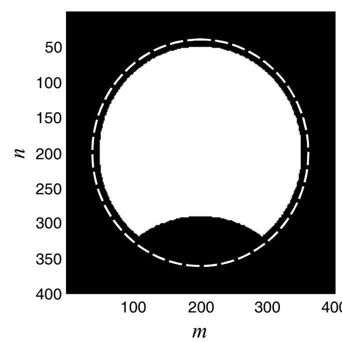

Figure 4. Correlation zone. The dashed line indicates the normalized area of the fingernail. The white area represents the subset that will be used for correlation.

Towards this end, a zone of correlation, **Z**, is first defined, which includes the normalized area of the fingernail with the lunular portion removed, as in Figure 4.

$$Z_{mn} = \begin{cases} 1 & \begin{array}{l} if\ [(m-200)^2 + (n-200)^2 < 150^2] \\ and\ [(m-450)^2 + (n-200)^2 > 160^2] \end{array} \\ 0 & \quad otherwise \end{cases} \tag{1}$$

The number of pixels in this area is given by:

$$N_{pix} = \sum_{m=1}^{400} \sum_{n=1}^{400} Z_{mn} = 52593 \tag{2}$$

Let **I** be the set of all images from all N_s=15 subjects for all N_p=8 poses. The image intensity for each ith subject and jth pose is normalized according to the average and standard deviation of the intensities in the correlation zone:

$$I'_{ijmn} = \frac{I_{ijmn} - \bar{I}_{ij}}{\sigma_{ij}} Z_{mn}$$

$$\bar{I}_{ij} = \frac{1}{N_{pix}} \sum_{m=1}^{400} \sum_{n=1}^{400} \left(I_{ijmn} Z_{mn} \right) \qquad \begin{matrix} i = 1,2 \ldots N_s \\ j = 1,2,\ldots N_p \end{matrix} \qquad (3)$$

$$\sigma_{ij} = \sqrt{\frac{\sum_{m=1}^{400} \sum_{n=1}^{400} \left(I_{ijmn} - \bar{I}_{ij} \right)}{N_{pix} - 1}}$$

Let **A** be the set of average images in Figure 3:

$$A_{jmn} = \frac{1}{N_s} \sum_{i=1}^{N_s} I_{ijmn} \qquad j = 1,2 \ldots N_p \qquad (4)$$

A is also normalized by the averages and standard deviations of the intensities in the correlation zone:

$$A'_{jmn} = \frac{A_{jmn} - \bar{A}_j}{\sigma_{Aj}} Z_{mn}$$

$$\bar{A}_j = \frac{1}{N_{pix}} \sum_{m=1}^{400} \sum_{n=1}^{400} \left(A_{jmn} Z_{mn} \right) \qquad (5)$$

$$\sigma_{Aj} = \sqrt{\frac{\sum_{m=1}^{400} \sum_{n=1}^{400} \left(A_{jmn} - \bar{A}_j \right)}{N_{pix} - 1}}$$

The correlations for each i^{th} subject between each j^{th} pose and each k^{th} average image is now computed:

$$C_{ijk} = \frac{1}{N_{pix}} \sum_{m=1}^{400} \sum_{n=1}^{400} I'_{ijmn} A'_{kmn} \qquad \begin{matrix} i = 1,2,\ldots N_s \\ j = 1,2,\ldots N_p \\ k = 1,2,\ldots N_p \end{matrix} \qquad (6)$$

Then the average and standard deviations of the correlations across all the subjects is computed:

$$\bar{C}_{jk} = \frac{1}{N_s} \sum_{i=1}^{N_s} C_{ijk}$$

$$S_{jk} = \sqrt{\frac{\sum_{i=1}^{N_s} \left(C_{ijk} - \bar{C}_{jk} \right)}{N_s - 1}} \qquad (7)$$

To evaluate statistical significance, the t-distribution is used, where the t-values are given by [12]:

$$t_{jk} = \frac{\bar{C}_{jj} - \bar{C}_{jk}}{\sqrt{\frac{S_{jj}^2}{N_s} + \frac{S_{jk}^2}{N_s}}} \qquad (8)$$

In order to find the confidence levels for statistical significance, the degrees of freedom are computed [12]:

$$\nu_{jk} = \frac{\left(\frac{S_{jj}^2}{N_s} + \frac{S_{jk}^2}{N_s} \right)^2}{\frac{\left(\frac{S_{jj}^2}{N_s} \right)^2}{N_s - 1} + \frac{\left(\frac{S_{jk}^2}{N_s} \right)^2}{N_s - 1}} = \frac{(N_s - 1)\left(S_{jj}^2 + S_{jk}^2 \right)^2}{S_{jj}^4 + S_{jk}^4} \qquad (9)$$

The minimum degree of freedom for all jk pairs is $\nu = 15$, which gives a conservative 95% confidence level of $t < 1.75$ and a conservative 99% confidence level of $t < 2.60$. For those pairs with greater degrees of freedom, the confidence levels shift to slightly more generous values of 1.65 and 2.33.

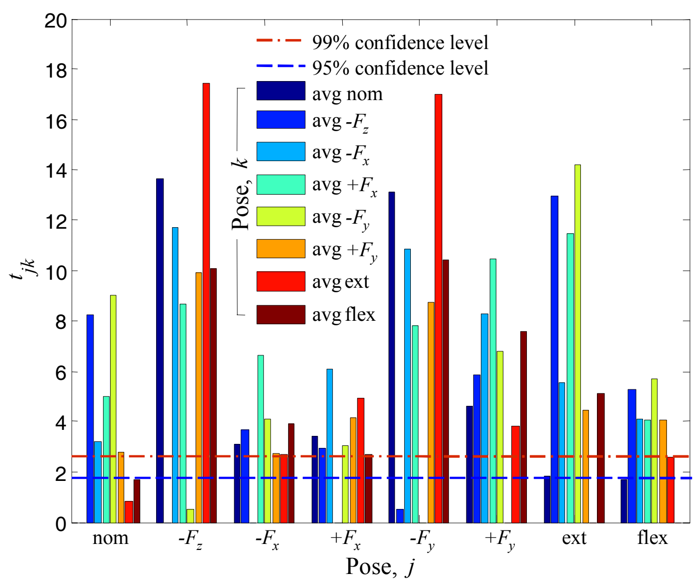

Figure 5. Statistical significance of coloration patterns. The t-value was computed for the correlations of each pose with true average image vs. the correlation with each of the other average images.

Figure 5 plots the t-values for the correlations and the minimum (most conservative) confidence levels. With the exception of -F_z and -F_y, all of the force poses correlate best to the average image of the true pose with better than 99% confidence. The two posture poses correlate best to themselves with better than 95% confidence. The patterns for -F_z and -F_y are on average too similar to each other, as one might suspect from a visible inspection of the images in Figure 3. Evidently, the addition of shear force in the negative *y*-direction does not change the coloration beyond what already occurs when a normal force is exerted downward in the *z*-direction. Also, the pattern for the nominal coloration of the nail is not significantly distinguishable from that of extension. However in this case, returning to the images in Figure 3, one may note that while the patterns for these two poses are similar, the brightness or intensity of the white zone appears to be much greater for extension. As a secondary means of distinguishing poses with similar patterns, the statistical significance of the average intensities in the white zones may be investigated. Two new zones corresponding to the distal and proximal regions of the fingernail are defined, illustrated in Figure 6.

$$\begin{aligned} &if\ [(m-250)^2+(n-200)^2>160^2] \\ &\qquad Zd_{mn}=Z_{mn} \quad and \quad Zp_{mn}=0 \\ &else \quad Zd_{mn}=0 \quad and \quad Zp_{mn}=Z_{mn} \end{aligned} \tag{10}$$

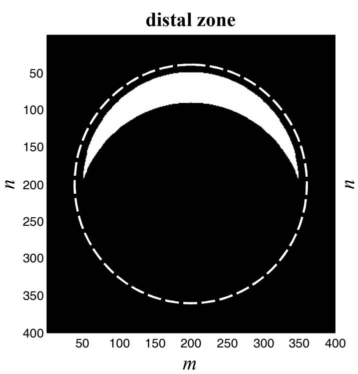

Figure 6. Distal and proximal zones of fingernail images. The white areas represent the subset areas of the normalized fingernail used to average intensities.

The average intensity for each i^{th} subject for each j^{th} pose within these two zones is computed:

$$D_{ij}=\frac{\sum_{m=1}^{400}\sum_{n=1}^{400}\left(I_{ijmn}Zd_{mn}\right)}{\sum_{m=1}^{400}\sum_{n=1}^{400}\left(Zd_{mn}\right)}, P_{ij}=\frac{\sum_{m=1}^{400}\sum_{n=1}^{400}\left(I_{ijmn}Zp_{mn}\right)}{\sum_{m=1}^{400}\sum_{n=1}^{400}\left(Zp_{mn}\right)} \tag{11}$$

and the average and standard deviation across the subjects:

$$\begin{aligned} \bar{D}_j&=\frac{1}{N_s}\sum_{i=1}^{N_s}D_{ij} & \bar{P}_j&=\frac{1}{N_s}\sum_{i=1}^{N_s}P_{ij} \\ SD_j&=\sqrt{\frac{\sum_{i=1}^{N_s}\left(D_{ij}-\bar{D}_j\right)}{N_s-1}} & SP_j&=\sqrt{\frac{\sum_{i=1}^{N_s}\left(P_{ij}-\bar{P}_j\right)}{N_s-1}} \end{aligned} \tag{12}$$

The *t*-values for the significances can then be computed using equations of the same form as (8) and (9) and are plotted in Figure 7 for the poses of interest. The nominal pose is now distinguishable from extension in terms of average intensity in the proximal zone with greater than 99% confidence.

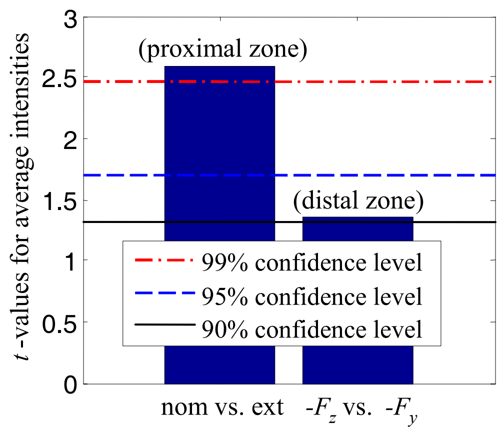

Figure 7. Statistical significance of average intensities. The *t*-values for the average intensity differences were computed for poses which did not have significantly different patterns. v = 27 for both.

For comparison, $-F_z$ and $-F_y$ are barely distinguishable with 90% confidence based on average intensities in the distal zone. If the $-F_y$ pose is removed from consideration, then it can be concluded that there are at least seven different poses that result in observable coloration patterns that are common to all subjects and distinct from each other with at least 95% confidence (>99% in most cases).

4. DISCUSSION

The preceding results serve as strong evidence that there is a set of characteristic color patterns that are representative of the population in general and are distinct for at least seven different poses of force and posture. In conjunction with continuing work [13][14], which show that individual variability and time dependence are not obstacles to distinguishing individual responses, this validates the potential of the fingernail sensor as a useful means for facilitating human-computer interaction (HCI) for people in general. At the very least, any user should be able to give six discrete commands (nominal pose would be a 7th null command) to the computer using the fingernail sensor, which for example, could be used to move a pointer, activate scroll bars, or navigate through menus. Results from previous work show that by calibrating the fingernail sensor to the individual user, we can go beyond discrete classification and estimate a continuous range of values of *x*, *y*, and *z* forces, as well as posture angle [10]. Because normal force and negative longitudinal shear do not result in a statistically significant difference in color, it may not be possible in general to independently recognize or estimate values of $-F_y$. This would place some constraints on the applications of the sensors to monitoring arbitrary grasping states of the fingers. However it would still allow for a variety of HCI applications where the mapping from sensor output to computer action could be tailored to available range of outputs. For example, horizontal motion of a computer pointer could be controlled by the entire range of *x*-forces, while the vertical motion is controlled by the positive range of *y*-forces or the negative range of *z*-forces, or some combination thereof.

Furthermore, the results of this paper in particular justify an effort to create a unified model of the color change mechanism that is applicable to people of various skin colors and fingernail sizes. This could be as simple as creating a set of average patterns that would allow the fingernail sensor to work on any person without calibration. Or it could be as complex as creating a physically-based model using the common anatomy and physiology of the fingertip that would explain how the various forces and postures create stress/strain fields within the fingertip. Preliminary research has begun towards creating such a unified physically-based model [15]. We anticipate that this model will help to understand what is mechanically transpiring inside the finger when various forces and posture are applied during various states of grasping and manipulation.

5. CONCLUSIONS

In conclusion, this paper presented an analysis of the photographically measured coloration patterns of the human fingernail for 15 subjects when various forces and postures are applied to the finger. The analysis indicates there are at least seven different states of fingertip force and finger posture that result in distinct fingernail coloration patterns that are common to all people according to a statistically significant measure.

In future work, we propose to develop a unified, physically-based model of the finger that explains the resulting blood perfusion patterns that occur in the fingernail bed when various forces and changes in posture are applied to the fingertip. Such a model will help to understand how various combinations of forces and postures create regions of compression and tension within the tissue under the fingernail that result in the visible patterns of reddening and whitening zones that are common to all people. This will be useful for designing future generations of fingernail sensors as well as for understanding human grasping and manipulation. Eventually, the effect of additional variables should be investigated, such as roll and pitch angles of the finger with respect to the surface, as well as variables that influence the cardiovascular state (e.g. temperature, hand elevation, heart rate, etc).

ACKNOWLEDGEMENT

This work was funded in part by the National Science Foundation, Grant: NSF IRI-0097700. Experiments in this work received IRB approval from the MIT Committee on the Use of Humans as Experimental Subjects (COUHES #2738).

REFERENCES

[1] Webster, J., ed., *Tactile Sensors for Robotics and Medicine*. New York: Wiley, 1988.

[2] Pawluk, D.T.V. and Howe, R.D., “Dynamic Lumped Element Response of the Human Fingerpad,” *J. Biomech. Eng.,* vol. 121, no. 2, pp. 178-183, 1999.

[3] Pawluk, D.T.V. and Howe, R.D., “Dynamic Contact of the Human Fingerpad Against a Flat Surface,” *J. Biomech. Eng.*, vol. 121, no. 6, pp. 605-611, 1999.

[4] Serina, E.R., Mote, C.D. Jr., and Rempel, D., “Force Response of the Fingertip Pulp to Repeated Compression—Effects of Loading Rate, Loading Angle, and Anthropometry,” *J. Biomechanics*, vol. 30, no. 10, pp. 1035-1040, 1997.

[5] Gulati, R.J., and Srinivasan, M.A., “Human Fingerpad under Indentation I: Static and Dynamic Force Response,” *ASME Bioengineering Conference*, BED-vol. 29, pp. 261-262, 1995.

[6] Singh, U. and Fearing, R.S., “Tactile After-Images from Static Contact,” *Proc. ASME Dynamic Systems and Control Division*, vol. 64, pp. 163-170, 1998.

[7] Han, H.-Y., Shimada, A., and Kawamura, S., “Analysis of Friction on Human Fingers and Design of Artificial Fingers,” *Proc. IEEE Int. Conf. on Robotics and Automation*, pp. 3061-3066, 1996.

[8] Scher, R.K. and Daniel, C.R. III, eds., *Nails: Therapy-Diagnosis-Surgery*. Philadelphia: W.B. Saunders, 2nd ed., 1997.

[9] Tubiana, R.T., ed., *The Hand*. Philadelphia: W.B. Saunders, vol. 1, 1981.

[10] Mascaro, S. and Asada, H., “Measurement of Finger Posture and Three-Axis Fingertip Touch Force Using Fingernail Sensors,” *IEEE Transactions on Robotics and Automation*, vol. 20, no. 1, pp. 26-35, 2004.

[11] Mascaro, S. and Asada, H., “Photoplethysmograph Fingernail Sensors for Measuring Finger Forces Without Haptic Obstruction,” *IEEE Transactions on Robotics and Automation*, vol. 17, no. 5, pp. 698-708, 2001,

[12] Weiss, N.A., and Hassett, M.J. *Introductory Statistics.* 2nd ed. Reading, Mass.: Addison-Wesley, 1987.

[13] Sun, Y., Hollerbach, J. and Mascaro, S., “Measuring Fingertip Forces by Imaging the Fingernail,” *Proc. 14th Int. Symp. Haptic Interfaces for Virtual Environment and Teleoperator Systems*, pp. 125-131, 2006.

[14] Sun, Y., Hollerbach, J. and Mascaro, S., “Dynamic Features and Prediction Model for Imaging Fingernail to Measure Finger Forces,” *Proc. IEEE Int. Conf. Robotics and Automation*, pp. 2813-2818, 2006.

[15] Mascaro, S. and Asada, H., “Understanding of Fingernail-Bone Interaction and Fingertip Hemodynamics for Fingernail Sensor Design,” *Proc. 10th Int. Symp. Haptic Interfaces for Virtual Environment and Teleoperator Systems*, pp. 106-113, 2002.